PROCEEDINGS OF SCIENCE

BSM scenarios with missing energy at future lepton colliders

Tania Robens[a,*]

[a] *Rudjer Boskovic Institute,*
Bijenicka cesta 54, 10000 Zagreb, Croatia

E-mail: trobens@irb.hr

I will briefly discuss the signatures and discovery prospects of several new physics models containing dark matter candidates at future lepton colliders. In particular, I will discuss the two models that, among other signatures, lead to electroweak gauge bosons and missing energy: the Inert Doublet Model, as well as the THDMa, a two Higgs doublet model with an additional pseudoscalar that serves as a portal to the dark sector. Results are mainly based on a Snowmass Whitepaper [1].
RBI-ThPhys-2022-42

41st International Conference on High Energy physics - ICHEP2022
6-13 July, 2022
Bologna, Italy

*Speaker

PoS(ICHEP2022)176

1. Introduction

I briefly discuss two models that enhance the scalar sector of the Standard Model by additional particle content, including dark matter candidates. These models lead to signatures with missing energy. I present current bounds on these models as well as perspectives and rates at future lepton colliders.

2. Inert Doublet Model

The Inert Doublet Model (IDM) [2–4] is a two Higgs Doublet Model (THDM) with a discrete exact $\mathbb{Z}_2$ symmetry containing a dark matter candidate.The model features 7 free parameters, which we chose in the so-called physical basis [5]: $v, M_h, M_H, M_A, M_{H^\pm}, \lambda_2, \lambda_{345}$, where the λs correspond to potential parameters. As two parameters (the vacuum expecation value (vev) v and $M_h \sim 125\,\text{GeV}$) are fixed by experimental measurements, we end up with a total number of 5 free parameters. Here, we consider the case where H is the dark matter candidate, which implies $M_{A,\,H^\pm} \geq M_H$.

The model is subject to a large number of theoretical and experimental constraints [1, 5–9]. These lead to a large reduction of the allowed parameter space. As an example, the masses are usually quite degenerate, as can be seen from figure 1[1]. We also consider the case when $M_H \leq$

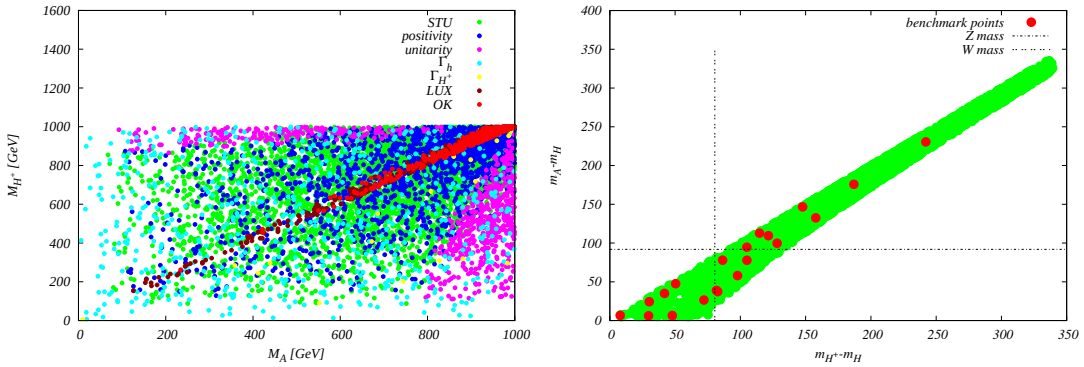

Figure 1: Masses are requested to be quite degenerate after all constraints have been taken into account. *Left:* In the $(M_A, M_{H^\pm})$ plane (taken from [5]). *Right:* In the $(M_{H^\pm} - M_H, M_A - M_H)$ plane (taken from [8]).

$M_h/2$, where constraints from $h \to$ invisible start to play an important role and an interesting interplay arises, between bounds from signal strength measurements, and bounds from dark matter relic density, see figure 2. In [5], it was found that this in general leads to a lower bound of $M_H \sim 50\,\text{GeV}$, with exceptions presented in [9]. The discovery potential of ILC and CLIC was investigated in [11–16] for several benchmark points proposed in [8], for varying center-of-mass energies from 250 GeV up to 3 TeV. We focus on AH and H^+H^- production with $A \to Z\,H$ and $H^\pm \to W^\pm H$, with leptonic decays of the electroweak gauge bosons. Event generation was done using WHizard 2.2.8 [17, 18], with an interface via SARAH [19] and SPheno 4.0.3 [20, 21] for model implementation. For CLIC results energy spectra [22] were also taken into account.

[1]Note that BP11 from [8] is by now excluded from the newest direct detection constraints [10].

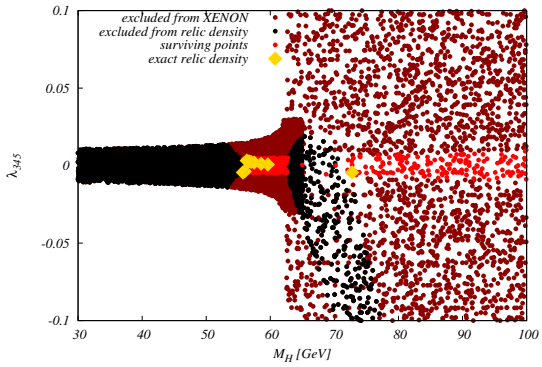

Figure 2: Interplay of signal strength and relic density constraints in the (M_H, λ_{345}) plane. Using XENON1T results, with golden points labelling those points that produce exact relic density (taken from [6]). Note that all points displayed here also pass the new LUX-Zeppelin bounds [10].

The investigated final states were $e^+e^- \to \mu^+\mu^- + \not{E}$, $e^+e^- \to \mu^\pm e^\mp + \not{E}$ for HA and H^+H^- production, respectively. Results for the discovery reach of CLIC, including center-of-mass energies of 1.5 TeV and 3 TeV, are shown in figure 3. In general, production cross sections $\gtrsim$ 0.5 fb and mass sums up to 1 TeV seem accessible, where the $\mu^\pm e^\mp$ channel seems to provide a larger discovery range.

3. THDMa

The THDMa is a type II two-Higgs-doublet model that is extended by an additional pseudoscalar a. In the gauge-eigenbasis, the additional scalar serves as a portal to the dark sector, with a fermionic dark matter candidate, denoted by χ. More details can e.g. be found in [23–29].

The model contains the following particles in the scalar and dark matter sector: h, H, $H^\pm$, a, A, χ. It depends on 12 additional new physics parameters

$$v,\, m_h,\, m_H, m_a, m_A,\, m_{H^\pm}, m_\chi;\ \cos(\beta-\alpha),\, \tan\beta, \sin\theta;\ y_\chi, \lambda_3, \lambda_{P_1},\, \lambda_{P_2},$$

where v and either m_h or m_H are fixed by current measurements in the electroweak sector.

I here report on results of a scan that allows all of the above novel parameters float in specific predefined ranges [29]. Two examples for direct bounds in 2-dimensional planes are displayed in figure 4. Note that for this proceeding, on contrast to the results presented in [1, 29], we have now updated the value of $B_s \to \mu^+\mu^-$ to the current PDG value [30], we have $B_s \to \mu^+\mu^- = (3.01 \pm 0.35) \times 10^{-9}$. Following the logic explained in [29], this leads to $(B_s \to \mu^+\mu^-)^{Spheno} \in [1.52; 3.34] \times 10^{-9}$. Note that the ΔM_s experimental value has also been updated [31] and now reads $\Delta M_s \left(\text{ps}^{-1}\right) = 17.765 \pm 0.004 \pm 0.004$. However, this basically leads to similar bounds as the previous value [32], so we did not update the respective bounds.

If, for consistency, now taking again a 3σ allowed range for $B_s \to \mu^+\mu^-$, the bounds from this branching ratio and ΔM_s basically overlapp. In turn, it means that now $\tan\beta$ values $\lesssim 1$ are still allowed. The second plot displays the relic density as a function of the mass difference $m_a - 2\,m_\chi$.

I also present cross section values for production at e^+e^- colliders for points that pass all bounds considered in [29] at a 3 TeV collider in figure 5.

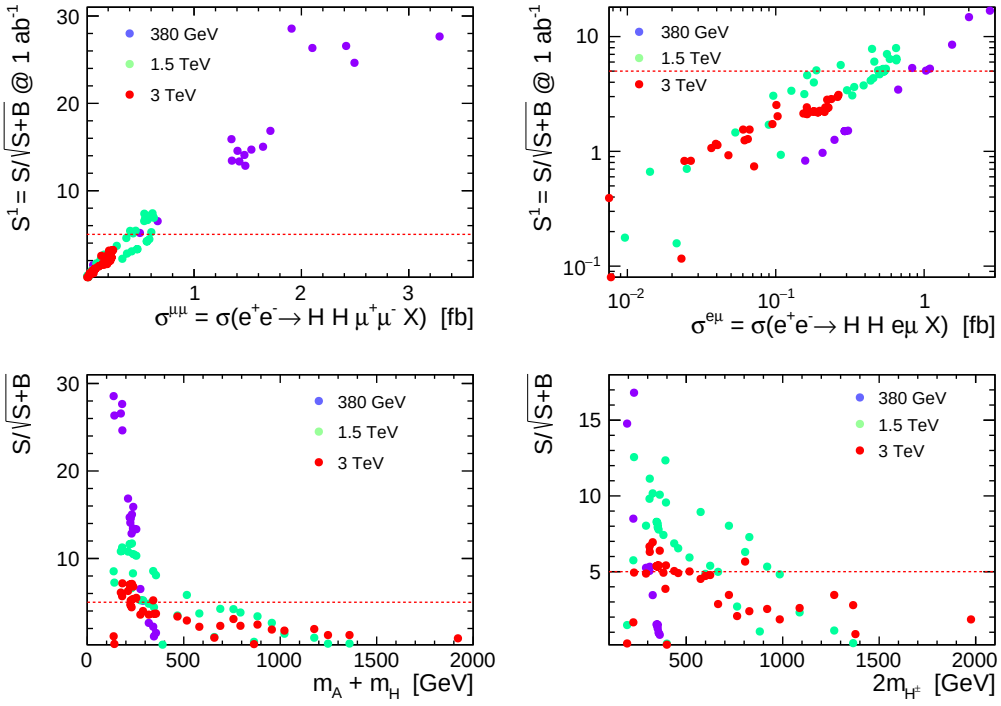

Figure 3: Discovery prospects at CLIC for the IDM in $\mu^+\mu^- + \not{E}$ *(left)* and $\mu^\pm e^\mp + \not{E}$ *(right)* final states, as a function of the respective production cross-sections *(top)* and mass sum of the produced particles *(bottom)*. Taken from [11].

4. Conclusion

I briefly presented two scenarios for models with dark matter candidates and their prospective signatures and rates/ discovery ranges at future lepton colliders, with a focus on larger ($\mathcal{O}$ (TeV)) center-of-mass energies. For the IDM, a detailed study shows that many still viable parameter points should be accessible, depending on the specifics of the particular benchmark points. For the THDMa, regions in parameter space exist where $t\bar{t} + \not{E}$ is the dominant production mode.

References

[1] J. Kalinowski, T. Robens, and A. F. Zarnecki, New Physics with missing energy at future lepton colliders - Snowmass White Paper, in *2022 Snowmass Summer Study*, 2022, 2203.07913.

[2] N. G. Deshpande and E. Ma, Phys. Rev. **D18**, 2574 (1978).

[3] Q.-H. Cao, E. Ma, and G. Rajasekaran, Phys. Rev. **D76**, 095011 (2007), 0708.2939.

[4] R. Barbieri, L. J. Hall, and V. S. Rychkov, Phys. Rev. **D74**, 015007 (2006), hep-ph/0603188.

[5] A. Ilnicka, M. Krawczyk, and T. Robens, Phys. Rev. D **93**, 055026 (2016), 1508.01671.

[6] A. Ilnicka, T. Robens, and T. Stefaniak, Mod. Phys. Lett. A **33**, 1830007 (2018), 1803.03594.

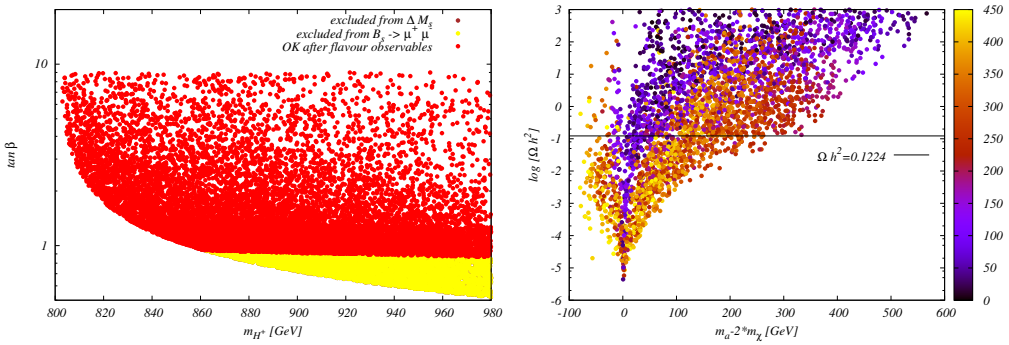

Figure 4: *Left:* Bounds on the $(m_{H^\pm}, \tan\beta)$ plane from B-physics observables, implemented via the SPheno [21]/ Sarah [33] interface, and compared to experimental bounds [34, 35]. The contour for low $\left(m_{H^\pm}, \tan\beta\right)$ values stems from [36, 37]. *Right:* Dark matter relic density as a function of $m_a - 2\,m_\chi$, with m_χ defining the color coding. The typical resonance-enhanced relic density annihilation is clearly visible. Right figure taken from [29].

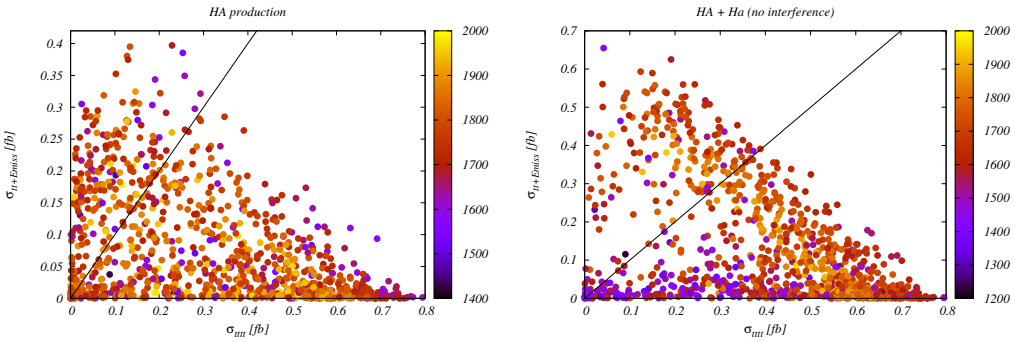

Figure 5: Production cross sections for $t\bar{t}t\bar{t}$ (x-axis) and $t\bar{t} + \not{E}$ (y-axis) final state in a factorized approach, for an e^+e^- collider with a 3 TeVcenter-of-mass energy. *Left:* mediated via HA, *right:* mediated via HA and Ha intermediate states. Color coding refers to $m_H + m_A$ *(left)* and $M_H + 0.5 \times (m_A + m_a)$ *(right)*. Figures taken from [29], with an update including results from [38].

[7] D. Dercks and T. Robens, Eur. Phys. J. C **79**, 924 (2019), 1812.07913.

[8] J. Kalinowski, W. Kotlarski, T. Robens, D. Sokolowska, and A. F. Zarnecki, JHEP **12**, 081 (2018), 1809.07712.

[9] J. Kalinowski, T. Robens, D. Sokolowska, and A. F. Zarnecki, Symmetry **13**, 991 (2021), 2012.14818.

[10] LZ, J. Aalbers *et al.*, (2022), 2207.03764.

[11] J. Kalinowski, W. Kotlarski, T. Robens, D. Sokolowska, and A. F. Zarnecki, JHEP **07**, 053 (2019), 1811.06952.

[12] CLIC, J. de Blas *et al.*, **3/2018** (2018), 1812.02093.

[13] A. F. Zarnecki *et al.*, PoS **ALPS2019**, 010 (2020), 1908.04659.

[14] A. F. Zarnecki *et al.*, Searching Inert Scalars at Future e^+e^- Colliders, in *International Workshop on Future Linear Colliders*, 2020, 2002.11716.

[15] D. Sokolowska *et al.*, PoS **EPS-HEP2019**, 570 (2020), 1911.06254.

[16] CLICdp, J. Klamka and A. F. Zarnecki, Eur. Phys. J. C **82**, 738 (2022), 2201.07146.

[17] M. Moretti, T. Ohl, and J. Reuter, p. 1981 (2001), hep-ph/0102195.

[18] W. Kilian, T. Ohl, and J. Reuter, Eur. Phys. J. **C71**, 1742 (2011), 0708.4233.

[19] F. Staub, Adv. High Energy Phys. **2015**, 840780 (2015), 1503.04200.

[20] W. Porod, Comput. Phys. Commun. **153**, 275 (2003), hep-ph/0301101.

[21] W. Porod and F. Staub, Comput. Phys. Commun. **183**, 2458 (2012), 1104.1573.

[22] L. Linssen, A. Miyamoto, M. Stanitzki, and H. Weerts, (2012), 1202.5940.

[23] S. Ipek, D. McKeen, and A. E. Nelson, Phys. Rev. **D90**, 055021 (2014), 1404.3716.

[24] J. M. No, Phys. Rev. **D93**, 031701 (2016), 1509.01110.

[25] D. Goncalves, P. A. N. Machado, and J. M. No, Phys. Rev. **D95**, 055027 (2017), 1611.04593.

[26] M. Bauer, U. Haisch, and F. Kahlhoefer, JHEP **05**, 138 (2017), 1701.07427.

[27] P. Tunney, J. M. No, and M. Fairbairn, Phys. Rev. **D96**, 095020 (2017), 1705.09670.

[28] LHC Dark Matter Working Group, T. Abe *et al.*, Phys. Dark Univ. **27**, 100351 (2020), 1810.09420.

[29] T. Robens, Symmetry **13**, 2341 (2021), 2106.02962.

[30] Particle Data Group, R. L. Workman *et al.*, PTEP **2022**, 083C01 (2022).

[31] HFLAV, Y. Amhis *et al.*, (2022), 2206.07501.

[32] HFLAV, Y. S. Amhis *et al.*, Eur. Phys. J. C **81**, 226 (2021), 1909.12524.

[33] F. Staub, Comput. Phys. Commun. **185**, 1773 (2014), 1309.7223.

[34] CMS-PAS-BPH-20-003, LHCb-CONF-2020-002, ATLAS-CONF-2020-049.

[35] HFLAV, Y. S. Amhis *et al.*, Eur. Phys. J. **C81**, 226 (2021), 1909.12524.

[36] M. Misiak, A. Rehman, and M. Steinhauser, JHEP **06**, 175 (2020), 2002.01548.

[37] M. Misiak, Private communication.

[38] CERN Report No., , 2021 (unpublished), ATLAS-CONF-2021-029.